

## ESTABLISHING AN EVOKED-POTENTIAL VISION-TRACKING SYSTEM

Trent A. Skidmore  
Ohio University  
Athens, Ohio

## SUMMARY

This paper presents experimental evidence to support the feasibility of an evoked-potential vision-tracking system. The topics discussed are stimulator construction, verification of the photic driving response in the electroencephalogram, a method for performing frequency separation, and a transient-analysis example. The final issue considered is that of object multiplicity (concurrent visual stimuli with different flashing rates). The paper concludes by discussing several applications currently under investigation.

## INTRODUCTION

The primary use of visual evoked potentials (VEPs) has been in clinical applications (refs. 1-2). However, because VEPs involve conceptually simple instrumentation, are relatively safe, and inherently noninvasive, they are worth investigating for possible use in other applications. One such application would be an evoked-potential vision-tracking system. To demonstrate the feasibility of such a system, it will be shown that distinct frequency-separable components can be evoked in the scalp potentials recorded using conventional electroencephalographic (EEG) techniques.

## THE STIMULATOR

A flexible stimulator was needed to investigate the issues involved in an evoked-potential interface. To realize the stimulator, a personal computer was used, equipped with the C programming language, a high-resolution video card and monitor. Several programs were generated that could flash a white object (either a square or arrow) on a black background at a specified rate. Computer hardware constrained the flashing rates to be integer submultiples of the 70.1 Hertz (Hz) screen update rate. This led to the four primary frequencies being 35.050, 23.367, 17.525, and 14.020 Hz. While slower flashing rates were possible, it was deemed that, at least for this initial investigation, a minimum of 14.020 Hz should be imposed. This was based primarily on the need to avoid the alpha band (8-13 Hz) and to minimize viewer irritation.

To ensure that the stimulator was performing as expected, data were collected using a photo darlington transistor. With the photo transistor taped to the monitor (stimulator), a 1" by 1" white square was flashed against a black background. For each of the chosen frequencies, the output of the photo transistor was seen to be a periodic train of pulses at the expected rate. Spectral analysis showed that each stimulating frequency produced a component at the fundamental as well as at higher harmonics. Thus, based on these findings, it was concluded that the stimulator was performing correctly, generating driving frequencies at the desired rates.

## VERIFYING THE PHOTIC DRIVING RESPONSE

To verify that the evoked potentials were detectable in the EEG, data were collected under five test conditions. These included flashing the 1" by 1" white square (at a viewing distance of 36") for two, sixteen-second runs at each of the rates listed above (35.050, 23.367, 17.525 and 14.020 Hz). In addition, to form a control set, data were collected for a run in which the subject looked at an illuminated black screen with no flashing object. The EEG was recorded (at a rate of 256 samples/second) over the O<sub>1</sub> and O<sub>2</sub> locations, each referenced to C<sub>z</sub>, according to the International 10-20 System of Electrode Placement. Sample spectra from the 35.050-Hz and 23.367-Hz runs are shown in figure 1, with the stimulating frequencies circled. To generate these plots, a hybrid periodogram was calculated. This periodogram averaged the spectra from both electrode pairs over two separate sixteen-second runs. This was done to highlight the peaks and to effectively reduce the surrounding noise. It is, however, crucial to note that the desired frequency peaks were also visible in the unaveraged spectra. The periodogram was performed merely to enhance the photic driving effect.

## FREQUENCY SEPARATION

To show that an evoked-potential interface is possible, it is important to verify that the four driving rates are distinguishable. To demonstrate this, sixteen seconds of O<sub>1</sub>-C<sub>z</sub> data for each rate were passed through four separate band-pass filters. The filters were fourth-order, infinite-impulse response Butterworth filters implemented in the LabVIEW programming language. The bandwidth of each filter was 1 Hz, with a center frequency corresponding to each driving rate (35.050, 23.367, 17.525 or 14.020 Hz). The spectral output of two of these filters is shown in figure 2. The legend indicates the notation used for each photic driving frequency. In both plots it is clear that the particular driving frequency being tested produces the largest spectral output. For example, in the top graph, data from the four rates were passed through the 35.050-Hz filter. As can be seen, the run containing the 35.050-Hz driving frequency, marked with the solid squares, has the largest spectral component at the output of the 35.050-Hz band-pass filter. In every case, each driving frequency produced the largest response in its associated filter.

From these results it is apparent that band-pass filtering can be used to detect the dominant frequency in the steady-state evoked potential. While it is beyond the scope of this paper to discuss frequency

detection schemes in detail, it has been demonstrated that separation and detection of the dominant photic driving frequency are possible.

## TRANSIENT ANALYSIS

To demonstrate the transient nature of the eye/brain system as the frequency of a single stimulating object is varied, it was necessary to devise a method for measuring time-dependent frequency changes. One manner of doing this is through the use of the spectrogram technique. To understand the operation of the spectrogram, suppose that a signal consists of the following components,

$$\begin{array}{ll}
 x(t) &= 0 & 0 < t < 4 \text{ seconds} \\
 &= 4 \cos(2\pi(10)t) & 4 < t < 8 \text{ seconds} \\
 &= 3 \cos(2\pi(20)t) & 8 < t < 12 \text{ seconds} \\
 &= 2 \cos(2\pi(30)t) & 12 < t < 16 \text{ seconds} \\
 &= 1 \cos(2\pi(40)t) & 16 < t < 20 \text{ seconds} \\
 &= 1 \cos(2\pi(30)t) & 20 < t < 24 \text{ seconds} \\
 &= 2 \cos(2\pi(20)t) & 24 < t < 28 \text{ seconds} \\
 &= 3 \cos(2\pi(10)t) & 28 < t < 32 \text{ seconds}
 \end{array}$$

and is sampled at 256 samples/second. A spectrogram of this signal is shown in figure 3. The plot consists of thirty-two one-second records or epochs. Each one-second record is the Fourier transform of a one-second block of time. The height of each record represents a linear measure of the spectral content during that particular time interval. The units on the horizontal axis are Hertz and the frequency binwidth (resolution) is 1 Hz. Observe from the example how the spectrogram plot "hides" lines of lower magnitude behind peaks that occur earlier in time. This convention allows time-dependent spectral trends to be observed while minimizing plot clutter.

The results of applying the spectrogram technique to demonstrate time-dependent spectral changes are highlighted in figures 4 and 5. Data for this test were collected when the stimulator was alternately flashing a 35.050-Hz and 23.367-Hz 1" white square on a black background. The stimulator initially displayed a brief message instructing the subject to watch the square. The stimulator then alternated between the two frequencies every five seconds. A total of forty-five one-second records are represented in the figures. The data was recorded over  $O_1$  with respect to  $C_Z$ .

To generate the spectrogram and to effectively illustrate the transitions between frequencies, the data were first passed through a parallel-filter network. This network consisted of two band-pass filters centered at 35.050 Hz and 46.733 Hz. The bandwidth of each filter was 4 Hz. The 35.050-Hz filter was used to isolate the 35.050-Hz component and a 46.733-Hz filter was used to isolate the 23.367-Hz component. The reason for using the 46.733-Hz filter is twofold: For this subject, the 23.367-Hz stimulator actually produced more distinct spectral peaks at the first harmonic (46.733 Hz) than at the fundamental. Furthermore, because of the 1-Hz binwidth limitation of this particular test, the 46.733-Hz

filter captured the 23.367-Hz stimulator effect better than a 23-Hz filter.

To further illustrate the transient effects, consider figure 5. These graphs show two frequency-slices from the spectrogram of figure 4. The top graph illustrates the spectral changes in the 35-Hz bin. The bottom graph illustrates the spectral changes in the 47-Hz bin. The numbers placed directly on the graphs indicate the fundamental stimulating component in that time range. For example, for  $1 \leq t \leq 5$  seconds, the stimulator was flashing 35.050 Hz. For  $6 \leq t \leq 10$  seconds, the stimulator was flashing 23.367 Hz, and so on. From these plots it is clear that the evoked-potential method can track time-dependent spectral changes as perceived by the eye/brain system. Furthermore, it is apparent that harmonics of the stimulating frequency are also of importance and may be of use in certain detection schemes.

## OBJECT MULTIPLICITY

Object multiplicity is the problem of having more than one flashing region within the field of vision. In order to achieve a viable interface, it is necessary for the eye/brain system to be able to distinguish between various flashing objects. To investigate this concept, a simple test scenario was devised. In this test, the monitor was made to flash two horizontal arrows, one at 35.050 Hz and the other at 23.367 Hz. Figure 6 shows the dimensions and spacing of the arrows. The viewing distance was again 36". Figure 7 shows the spectral results when the horizontal separation  $\{s\}$  of the arrows was 3.5". For the upper graph, the subject was instructed to look at the 35.050-Hz arrow (placed at screen right). As expected, there is a large spectral peak at this frequency and no significant 23.367-Hz component. The lower graph shows the spectrum generated when the subject was focused on the 23.367-Hz flashing arrow. Note that the dominant peak is again at the driving frequency under observation.

To further test the object-multiplicity issue, the arrows were moved to a separation of only 1.75". The results from this test were similar to those described above. As a final test, the arrows were flashed with no horizontal separation  $\{s=0\}$ . Again, the driving frequencies were surprisingly distinguishable. Therefore, based on these results, the eyes appear to be able to focus on a region that is sufficiently small so as to allow this type of system to be used in a direct human-computer interface.

## APPLICATIONS

There are many possible applications for an evoked-potential vision-tracking system. Two applications that are currently being investigated include a two-dimensional directional controller (fig. 8), and a moving-target tracking system (fig. 9). In the figure-8 scenario, the user observes and watches a stimulator that is displaying a four-arrow arrangement. Each arrow is flashed at a different frequency. This is done in order to evoke a frequency-separable photic driving response that is dependent upon which arrow the subject is looking at. For example, if the subject is focusing on the "up" arrow, flashing at a frequency of  $f_1$  (flashes per second), then an  $f_1$ -Hz component should manifest itself in the EEG.

Subsequently, if the user changes focus from the "up" arrow to, say the "right" arrow, then the primary frequency being driven into the EEG will be changed from  $f_1$  to  $f_2$ . Using a detector that would recognize these frequency changes, a user could systematically focus on a particular sequence of arrows to perform a two-dimensional control task, such as moving a computer's mouse.

Figure 9 illustrates one possible realization of a moving-target tracking system. For this, the user would watch a monitor (stimulator) displaying, for example, several moving airplanes, each flashing at different rates. Upon determining which airplane the user was focused on, the computer would highlight that plane. Based solely on the photic driving response of the highlighted object, the application would be capable of tracking the eye's movement as the airplane (target) moves across the screen.

## CONCLUSIONS

Several important issues have been discussed that relate to the feasibility of an evoked-potential vision-tracking system. It has been shown that the photic driving response is apparent in the spectra of the EEG and is distinguishable through band-pass filtering. It has also been shown that the transient properties of the photic driving response are well defined, indicating that the eye/brain system is capable of discerning time-dependent frequency changes. Finally, it has been demonstrated that dual stimulating objects also appear to generate responses that are unique and separable. Based on these results, a conceptual foundation for a vision-based interface has been established.

## ACKNOWLEDGEMENT

The work reported here was in part funded through NASA Grant NAG 1-940 and is the subject of a patent disclosure (No. 18/4/91) filed at Ohio University April 9, 1991.

## REFERENCES

1. Barber, C. and Blum, T. eds.: Evoked Potentials III - The Third International Evoked Potentials Symposium, 1987.
2. Bodis-Wollner, I. ed.: Evoked Potentials, Annals of The New York Academy of Sciences, Vol. 388, 1982.

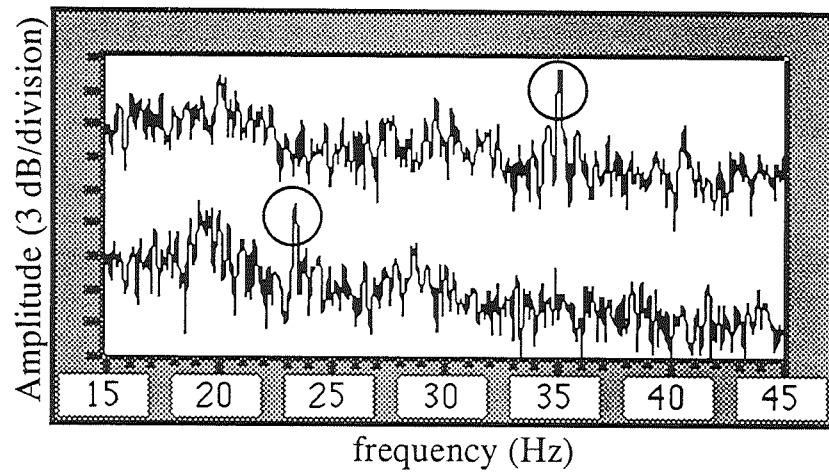


Figure 1. Photic Driving Response at 35.050 and 23.367 Hz.

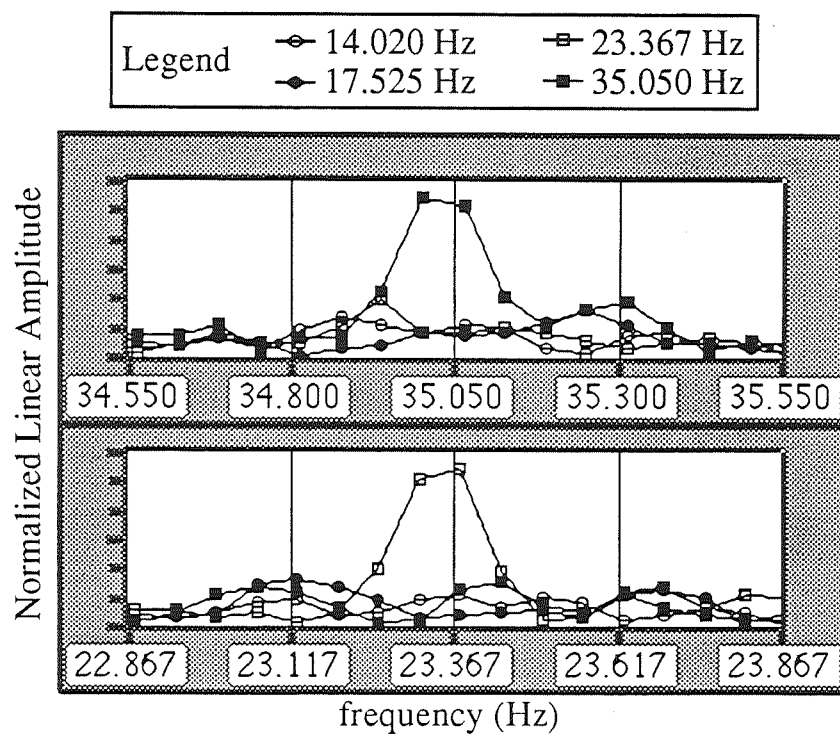


Figure 2. Frequency Separation Using Band-Pass Filtering.

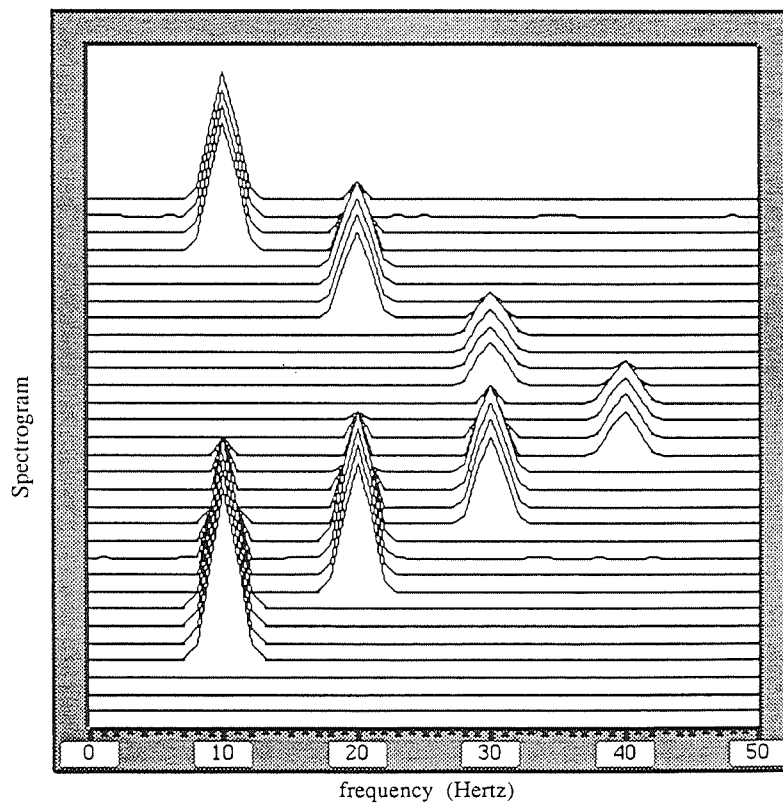


Figure 3. Spectrogram example.

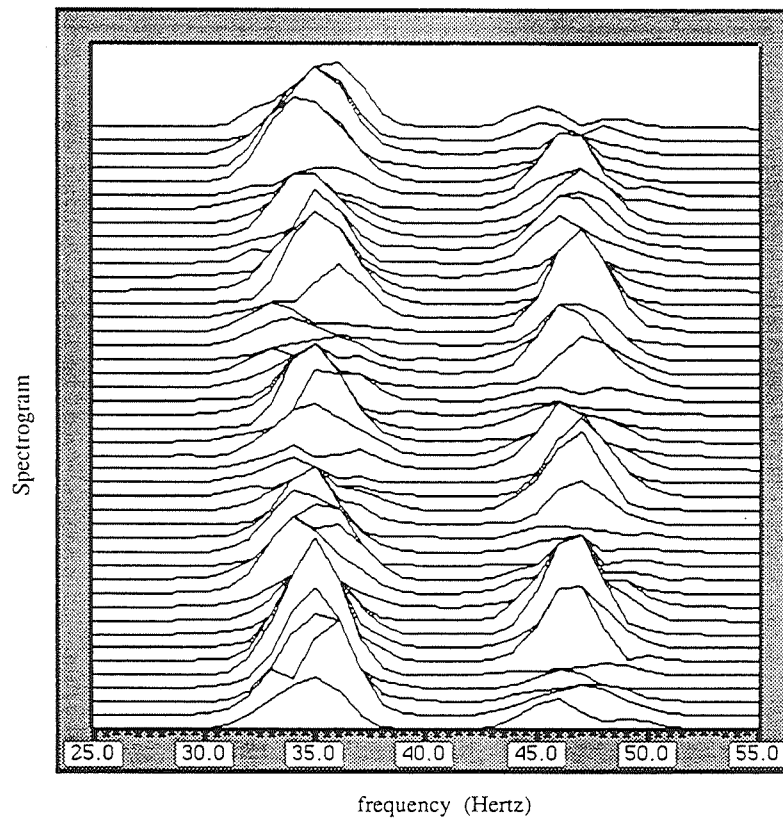


Figure 4. Spectrogram for the output of 35- and 47-Hz band-pass filters.

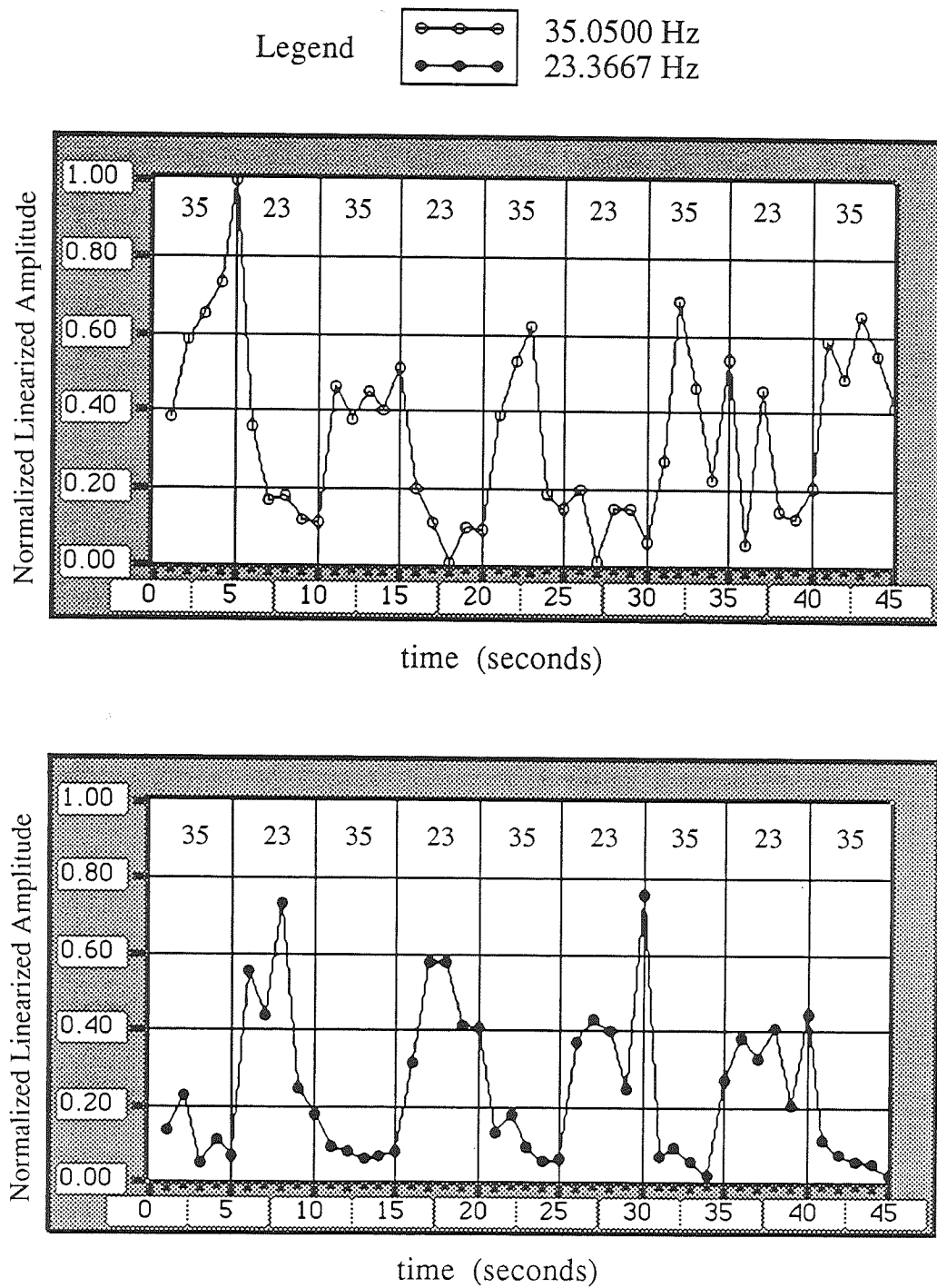


Figure 5. 35-Hz (top) and 47-Hz (bottom) spectrogram slices.



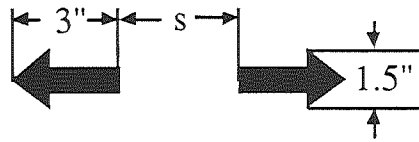


Figure 6. Object Multiplicity Test.

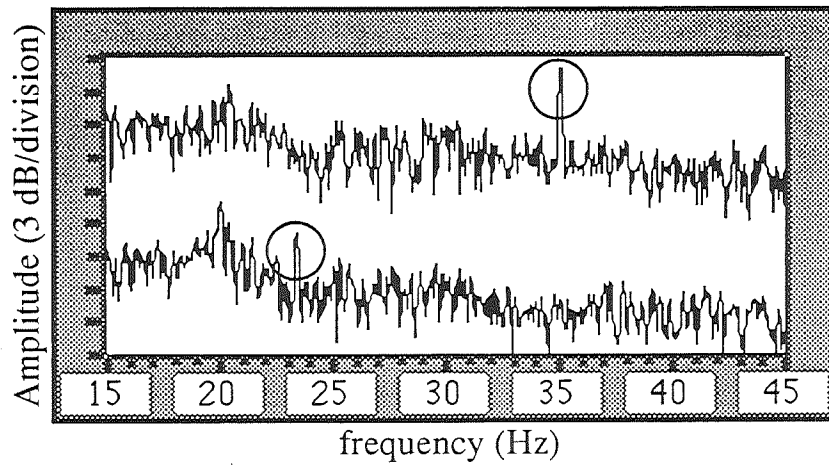


Figure 7. Object Multiplicity at 35.050 and 23.367 Hz.

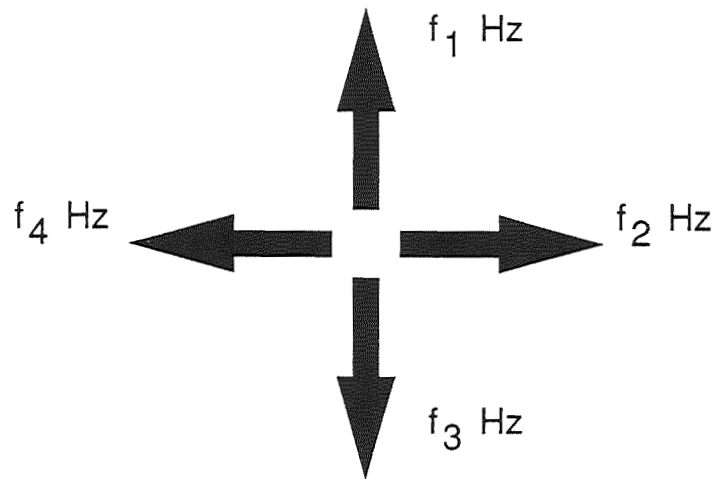


Figure 8. Four-arrow evoked-potential interface.

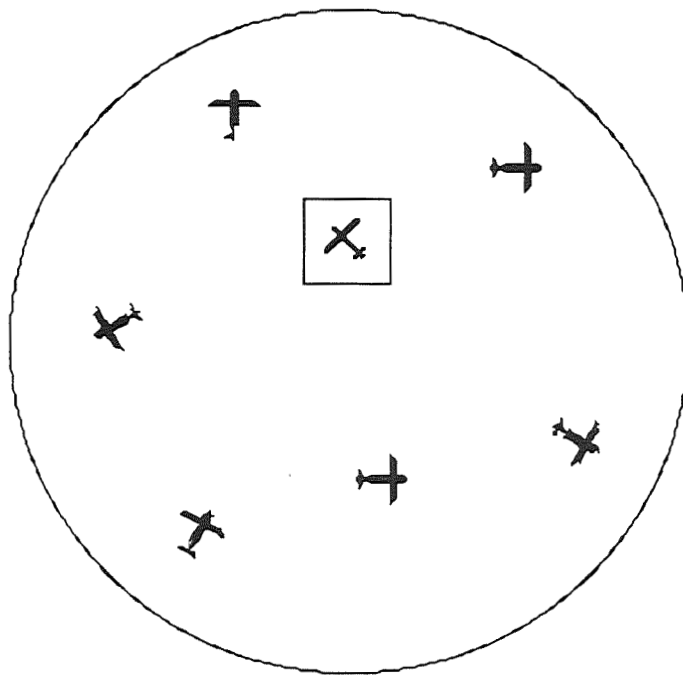


Figure 9. The target-tracking evoked-potential interface.